MucosalImmunology www.nature.com/mi

ARTICLE

Subcellular antigen localization in commensal *E. coli* is critical for T cell activation and induction of specific tolerance

Eveline Bennek[1], Ana D. Mandić[1], Julien Verdier[1], Silvia Roubrocks[1], Oliver Pabst[2], Niels Van Best[3], Inga Benz[4], Thomas Kufer[5], Christian Trautwein[1] and Gernot Sellge[1]

Oral tolerance to soluble antigens is critically important for the maintenance of immunological homeostasis in the gut. The mechanisms of tolerance induction to antigens of the gut microbiota are still less well understood. Here, we investigate whether the subcellular localization of antigens within non-pathogenic *E. coli* has a role for its ability to induce antigen-specific tolerance. *E. coli* that express an ovalbumin (OVA) peptide in the cytoplasm, at the outer membrane or as secreted protein were generated. Intestinal colonization of mice with non-pathogenic *E. coli* expressing OVA at the membrane induced the expansion of antigen-specific Foxp3$^+$ T_{regs} and mediated systemic immune tolerance. In contrast, cytoplasmic OVA was ignored by antigen-specific CD4$^+$ T cells and failed to induce tolerance. In vitro experiments revealed that surface-displayed OVA of viable *E. coli* was about two times of magnitude more efficient to activate antigen-specific CD4$^+$ T cells than soluble antigens, surface-displayed antigens of heat-killed *E. coli* or cytoplasmic antigen of viable or heat-killed *E. coli*. This effect was independent of the antigen uptake efficiency in dendritic cells. In summary, our results show that subcellular antigen localization in viable *E. coli* strongly influences antigen-specific CD4$^+$ cell expansion and tolerance induction upon intestinal colonization.

Mucosal Immunology (2019) 12:97–107; https://doi.org/10.1038/s41385-018-0061-0

INTRODUCTION

The intestinal immune system needs to maintain immune homeostasis despite the presence of a large amount of potentially harmful commensal bacteria and high loads of dietary antigen. Disruption of this immunological balance can lead to diseases like inflammatory bowel disease and food allergy.[1–4]

Intestinal dendritic cells (DCs) have a unique potential to induce the development of regulatory T cells (T_{regs}) under non-inflammatory conditions.[5] Therefore, oral uptake of soluble antigens induces a systemic non-responsiveness to the respective antigen.[6,7] The intestinal microbiota triggers both T_{regs} or effector T cells,[8–12] which on the one hand protects from excessive immune reactions and on the other hand induces a subinflammatory immune response controlling unlimited growth of microbiota at the gastrointestinal barrier.[13,14] It has been suggested that commensals that can adhere to intestinal epithelial cells, such as *Segmented filamentous bacteria*, predominantly trigger Th17 cells.[8,15] In contrast, multiple other strains or mixtures of strains with a predominantly luminal localization such as *Clostridia* belonging to the clusters IV, XIVa and XVIII,[11,16,17] Polysaccharide A-expressing *Bacteroides fragilis*,[18] *Bifidobacteria*,[19] and altered Schaedler's flora[20] induce the development of T_{regs}. T_{regs} may be largely non-specifically induced by bacterial metabolites such as short-chain fatty acids,[21,22] yet microbiota-specific T_{reg} have been reported.[17,23] What determines their antigen-specificity is only poorly known and is a major challenge for potential future immunotherapy approaches.

The objective of the current study was to investigate whether the subcellular antigen localization within a commensal has a role for the ability to trigger immune tolerance or active immunity. The hypothesis was that secreted antigens or antigens derived from degraded microbiota within the lumen might be most effective in inducing tolerance. These antigens may be recognized in a similar way as food antigens that are efficient in driving oral tolerance. For example, colonization with *Lactococcus lactis* secreting ovalbumin (OVA) induces an OVA-specific tolerance in mice.[24] In contrast, antigens that remain associated with bacteria and their microbe-associated molecular patterns (MAMPs) may have the potential to change the activation state of intestinal antigen-presenting cells (APCs). Antigens associated with TLR agonists in the same phagolysosome has been shown to more efficiently prime effector T cells than antigens and TLR agonists in a non-associated form.[25]

We generated non-pathogenic *E. coli* that express an OVA peptide in the cytoplasm, at the outer membrane or as secreted protein. The outer membrane-embedded AIDA-I Transporter (adhesin involved in diffuse adherence) served as a surface-display system for this purpose.[26] After intestinal colonization of the different OVA-expressing and control *E. coli* strains, we studied activation of antigen-specific FoxP3$^+$ T_{regs} and systemic tolerance induction in an OVA-specific allergic lung inflammation model. In disagreement with our hypothesis not soluble but surface-displayed antigens were most efficient in expanding antigen-specific FoxP3$^+$ T_{regs} and inducing systemic tolerance. Mechanistically, this result could be explained by the fact

[1]Department of Internal Medicine III, University Hospital RWTH Aachen, Aachen, Germany; [2]Institute of Molecular Medicine, University Hospital RWTH Aachen, Aachen, Germany; [3]Institute of Medical Microbiology, University Hospital RWTH Aachen, Aachen, Germany; [4]Zentrum für Molekularbiologie der Entzündung (ZMBE), Institut für Infektiologie, Westfälische Wilhelms-Universität, Münster, Germany and [5]Department of Immunology, Institute of Nutritional Medicine, University of Hohenheim, Stuttgart, Germany
Correspondence: Gernot Sellge (sellge@gmx.de)

Received: 11 June 2017 Revised: 17 June 2018 Accepted: 23 June 2018
Published online: 16 October 2018

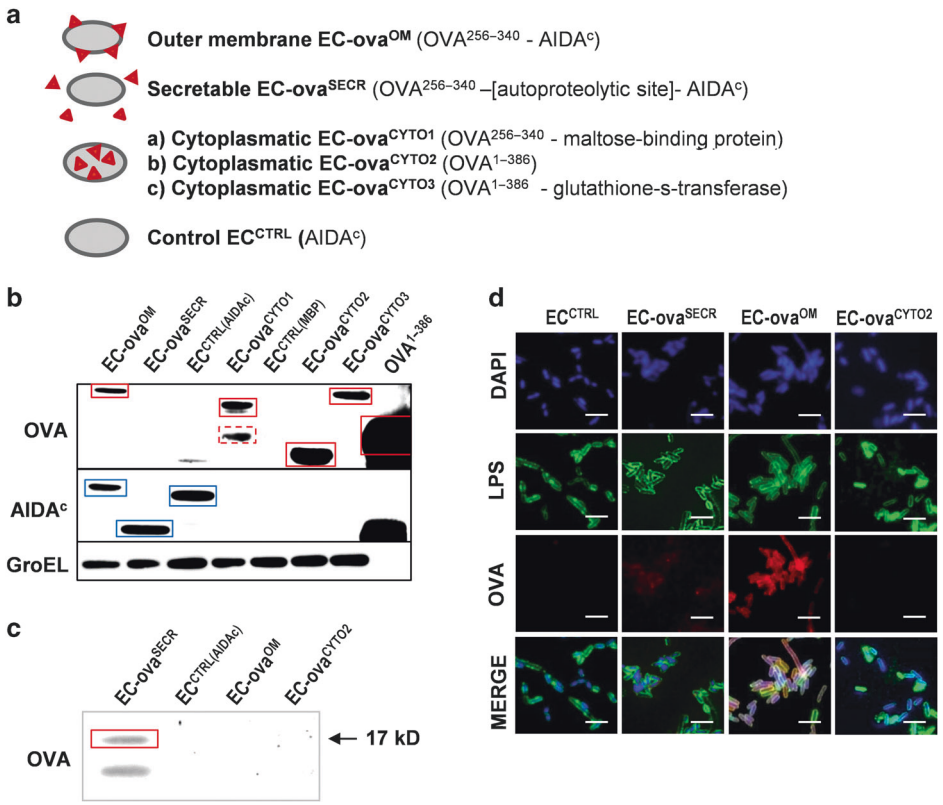

Fig. 1 Generation of *E. coli* expressing OVA in different cellular compartments. **a** Schematic illustration of different OVA-expressing *E. coli* strains. For details see also Supplementary Figure 1. **b** WB analysis with Abs specific for OVA, AIDA^{c}, and GroEL of indicated strain lysates. Bacterial chaperon GroEL was used as loading control and sOVA as positive control. Boxes indicate proteins of the expected size. Box with dashed line indicates a spliced protein in EC-ova^{CYTO1}. EC$^{CTRL(MBP)}$ expresses MBP without inserted OVA peptide. **c** WB of trichloroacetic acid concentrated culture supernatants of indicated strains with an OVA-specific Ab. **d** IF for OVA (red), LPS (green), and DAPI staining (blue) of indicated strains. Bar represents 5 µm

that membrane-associated antigens of viable *E. coli* were about two times of magnitude more efficient to activate antigen-specific CD4^{+} T cells than soluble antigens, surface-displayed antigens of heat-killed *E. coli* or cytoplasmic antigens of live or dead *E. coli*.

RESULTS

Generation of *E. coli* expressing OVA in different cellular compartments

We generated *E.coli* strains with a streptomycin-resistant *K12* background that express a 85 amino acid (aa) fragment (256–340) of OVA containing the main epitopes for T cell recognition.[27] The localization of the OVA peptide was designed to be expressed and retained in the cytoplasm (fused to maltose binding protein [MBP] in EC-ova^{CYTO1}) or presented at the outer membrane (fused to AIDA^{c} in EC-ova^{OM}). In EC-ova^{SECR}, AIDA^{c} contains an autoproteolysis motif leading to cleavage and release of the fused OVA peptide.[26] Furthermore, intracellular full length OVA (1–386) was expressed alone (EC-ova^{CYTO2})[28] or fused to glutathione-*s*-transferase (EC-ova^{CYTO3}).[29] *E. coli* expressing AIDA^{c} without an OVA fragment (EC^{CTRL}) was used as a negative control (Fig. 1a and Supplementary Figure 1). All plasmids contained a gene coding for ampicillin resistance.

OVA was detected in bacterial lysates of EC-ova^{OM} and EC-ova$^{CYTO1/2/3}$ (Fig. 1b), and cleaved OVA peptides produced by EC-ova^{SECR} were detected in culture supernatants (Fig. 1c). OVA expression in EC-ova^{CYTO2} and EC-ova^{CYTO3} was observed despite the absence of IPTG induction, reflecting leakiness of the lac repressor system. Since we aimed to compare *E. coli* with similar expression levels of OVA, we conducted all subsequent experiments without IPTG induction. The bands for AIDA^{c} in EC-ova^{SECR} and EC-ova^{OM} indirectly indicate similar OVA expression by both strains. Size difference of AIDA^{c} was due to the cleavage of the secreted OVA fragment (Fig. 1b). Immunofluorescence (IF) staining proved membranous AIDA^{c} expression in EC-ova^{SECR} and EC-ova^{OM} (Supplementary Figure 2B) and membranous OVA expression in EC-ova^{OM} (Fig. 1d). A weak OVA signal at the surface of EC-ova^{SECR} might indicate OVA peptides retained in the outer membrane. The absence of OVA detection in EC-ova$^{CYTO1/2/3}$ is due to the impermeability of bacterial cell walls to Abs[30] (Fig. 1d and Supplementary Figure 2B).

Colonization with EC-ova^{OM} and EC-ova^{SECR} induces an OVA-specific immune tolerance in mice

After intragastric gavage of ampicillin-resistant *E. coli* K12, colonization till day 21 was maintained when ampicillin was present in drinking water. Median CFU counts in fecal pellets were 6.9×10^{8} per gram feces (range 3.7×10^{6}–2.1×10^{10}) corresponding to a median relative abundance of 1.02% (range 3.2×10^{-4}–36.9%; Supplementary Figure 3). As observed in physiological conditions,[31] colonization density increased from the proximal to the distal part of the gut and translocation of live bacteria to mesenteric lymph nodes (MLNs), spleen and liver was occasionally detectable (Fig. 2a). Colonized mice did not show any sign of intestinal inflammation or changes in body weight compared to control mice treated with ampicillin without gavage of *E. coli* (Fig. 2b and Supplementary Figure 4). IF staining of colonic sections confirmed stable OVA surface expression in

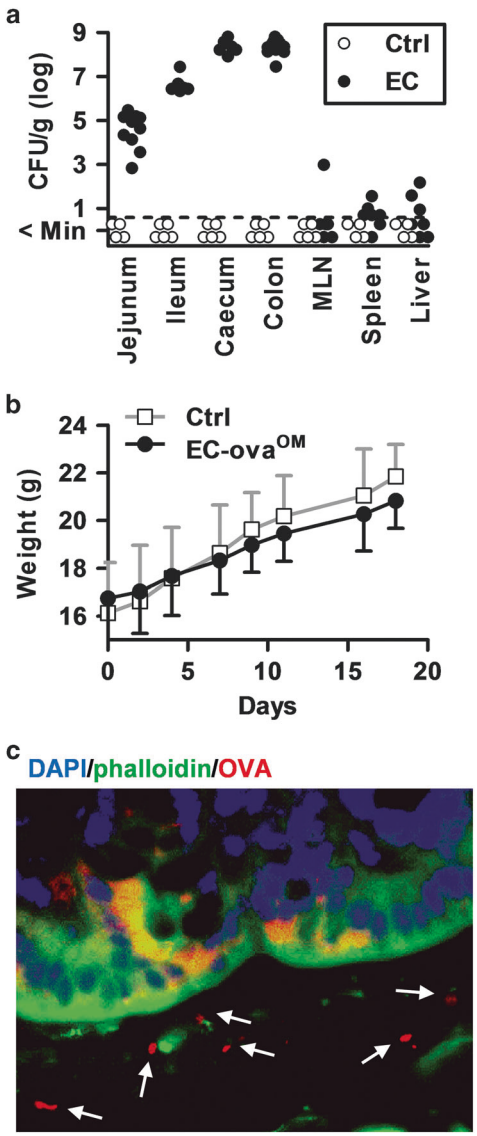

Fig. 2 Intestinal colonization of mice with *E. coli K12*. Mice received 1 g/L ampicillin in the drinking water from day −1 till the end of the experiment. At day 0 and 7 mice were intragastrically gavaged with 10^9 ampicillin/streptomycin-resistant EC^{CTRL} or EC-ova^{OM} as indicated. Control mice (Ctrl) received ampicillin in the drinking water without gavage of *E. coli*. **a** Stool homogenates of EC^{CTRL} colonized mice were cultured on ampicillin/streptomycin agar plates to determine CFU per gram of intestinal content from indicated locations and per total organ (MLNs, spleen, liver) at day 5. Each dot represents one mouse. **b** Weight development in EC-ova^{OM} colonized and control mice (mean ± SEM; $n = 4$ per group). Like EC-ova^{OM} none of the other *E. coli* strains used in this study caused weight loss upon colonization (data not shown). **c** Representative IF of a carnoy-fixed colon section from Ec-ova^{OM} colonized mice at day 21 stained for OVA (red), phalloidin (green), and DAPI (blue). Sections from control mice did not show OVA-positive bacteria (data not shown)

EC-ova^{OM} at day 21 of colonization. OVA signal was almost exclusively found in the lumen (Fig. 2c).

To investigate the capacity of OVA-producing *E. coli* strains to induce OVA-specific tolerance, we used a model of OVA-induced allergic lung inflammation (Fig. 3a). All OVA-expressing *E. coli* strains and EC^{CTRL} had a similar colonization efficacy (Supplementary Figure 3). Colonization of *E. coli* without OVA expression (EC^{CTRL}) did not significantly influence allergic airway inflammation (Supplementary Figure 5). As a positive control of oral tolerance induction, EC^{CTRL}-colonized mice were fed with soluble OVA (sOVA). Colonization with EC-ova^{OM} or EC-ova^{SECR} significantly decreased OVA-induced allergic lung inflammation as compared to colonization with EC^{CTRL}. We found decreased numbers of eosinophils, $CD4^+$ and $CD8^+$ T cells in bronchoalveolar lavage (BAL) fluids (Fig. 3b), lower mRNA expression of the Th2-type cytokines *Il4* and *Il13* in lung tissue (Fig. 3c), and decreased edema and presence of inflammatory infiltrates within the alveolar tissue (Fig. 3d). In contrast, colonization with EC-$ova^{CYTO1/2/3}$ did not influence OVA-induced allergic lung inflammation (Fig. 3b–d).

These results suggest that subcellular antigen localization in gut commensals have a major role for the ability to induce antigen-specific immune tolerance.

Tolerance induction by EC-ova^{OM} and EC-ova^{SECR} is associated with the expansion of antigen-specific T_{regs} in vivo

Specific immunotherapy for allergies induce IgG-blocking Abs that mask IgE-binding epitopes and co-engage inhibitory Fcγ receptors IIb on mast cells (MCs) or basophils,[4] and induces the activation of antigen-specific T_{regs}.

To test a potential impact of OVA-specific blocking antibodies, we quantified OVA-specific IgG1 and IgG2b Abs in sera and performed an in vitro MC degranulation assay. Anti-OVA IgG1 Abs were detectable in sera of most animals after induction of OVA-specific lung inflammation; however, no significant differences were observed between the experimental groups. OVA-specific IgG2b Abs were only significantly induced in sOVA-fed mice, whereas they were only occasionally present in other groups (Supplementary Figure 7A). Functional testing revealed that none of the different sera had the capacity to inhibit antigen-specific degranulation of mast cells in vitro (Supplementary Figure 7B) suggesting that blocking Abs do not have a major role in driving the observed tolerance induced by colonization with EC-ova^{OM} and EC-ova^{SECR}.

To study the expansion of T_{regs}, we adoptively transferred CFSE-labeled OVA-specific transgenic OTII $CD4^+$ cells to mice colonized subsequently with EC-ova, EC^{CTRL} or fed with sOVA as positive control. We assessed clonal proliferation and FoxP3 expression in OTII cells derived from MLNs and spleens at day 20 (for protocol see Fig. 4a). Proliferation and FoxP3 expression above background (=EC^{CTRL}-colonized mice) was found in mice colonized with EC-ova^{OM} and EC-ova^{SECR}, but not in mice colonized with EC-$ova^{CYTO1/2/3}$ (Fig. 4b, c).

In summary, these results show that the ability of EC-ova^{OM} and EC-ova^{SECR} to induce antigen-specific systemic tolerance correlates with their capacity to expand antigen-specific $FoxP3^+$ T cells.

Antigen surface-display in association with bacterial viability confers highly efficient antigen-specific T cell activation in vitro

We studied whether the localization of antigen expression influence the ability of DCs to present OVA to OTII T cells. Bone marrow-derived DCs (BMDCs) were co-cultured with EC-ova or EC^{CTRL} for 90 min before removing supernatants and blocking residual extracellular growth with medium containing gentamycin. CFSE-labeled OTII cells were added and proliferation was analyzed by FACS after 4 days of co-culture.

Similar to what was observed in vivo, EC-ova^{OM} and to a slightly lesser extent EC-ova^{SECR}, but not EC-$ova^{CYTO1/2/3}$ induced proliferation of OTII cells in vitro (Fig. 5a). Dosing experiments revealed that an input of 5×10^6 live bacteria (~2×10^7 bacteria after 90 min when antibiotics were added) was the most efficient dose for inducing OTII cell proliferation. Higher doses were less efficient, which correlated with induction of T cell death at higher doses. Cell death was independent of the presence of OVA and was, therefore, most likely a toxic effect of live bacteria (Fig. 5b).

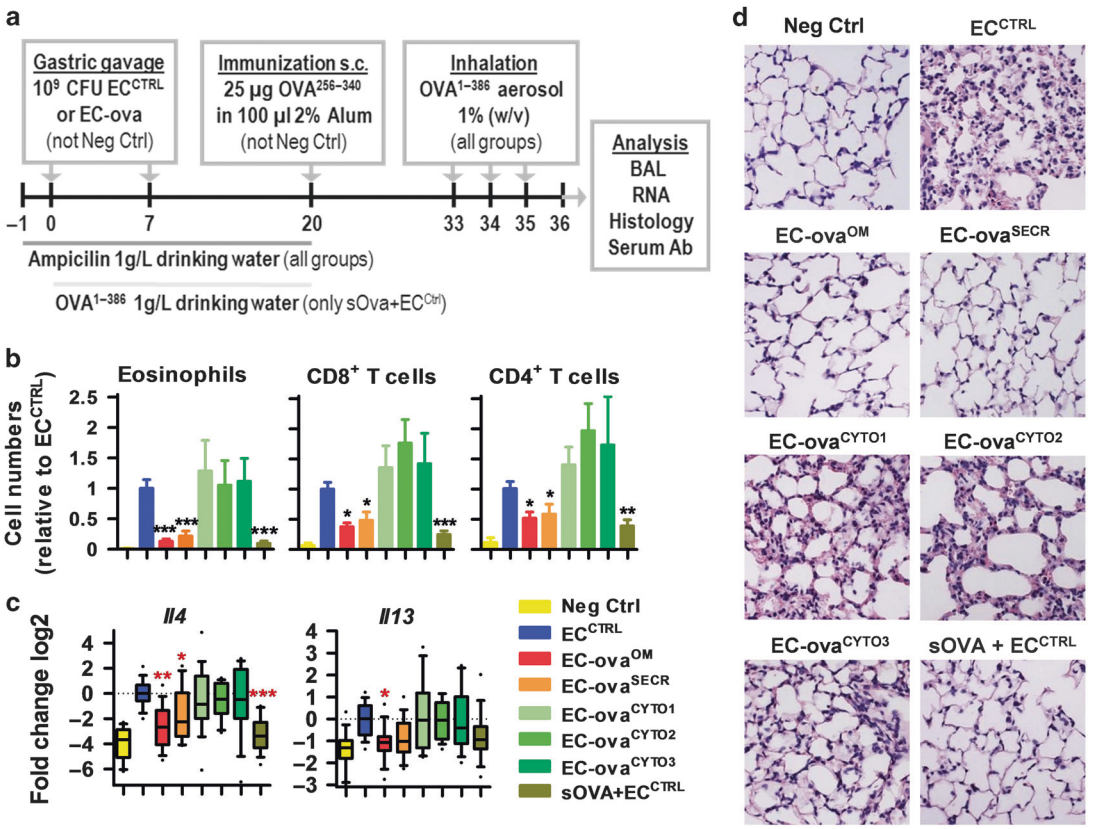

Fig. 3 Colonization with EC-ova^{OM} and EC-ova^{SECR} induces tolerance in an OVA-induced allergic lung inflammation model. **a** Experimental setup. **b** Eosinophil, CD4$^+$ and CD8$^+$ T cell numbers in BAL analyzed by FACS. For gating strategy see Supplementary Figure 6. Data are expressed as mean fold change ± SEM compared to EC^{CTRL}. **c** mRNA expression in lung tissue for *Il4* and *Il13* expressed as log2 fold change (FC) compared to log mean of the EC^{CTRL} condition. Boxes and whiskers indicate median, and 10/25/75/90 percentiles. **b**/**c** Data of 4 experiments with 4 mice per group, respectively, are shown (total $n = 16$ per group). Statistical differences were determined by one-way ANOVA following Dunn's post hoc test (test did not include Neg Ctrl). *$p < 0.05$; **$p < 0.01$; ***$p < 0.001$. **d** Representative H&E stained lung sections

Heat-killed (HK) EC-ova^{OM} and EC-ova^{SECR} were less efficient than viable bacteria. To induce the same rate of OTII proliferation about 100 times more HK *E. coli* than live *E. coli* were required. Unlike live bacteria, HK *E. coli* caused only a very low level of T cell death at higher doses (Fig. 5b). Interestingly, also HK EC-ova^{CYTO1} induced OTII proliferation even at about ten times lower concentrations ($=6 \times 10^7$) than HK EC-ova^{OM} and EC-ova^{SECR}. Bacterial lysates, OMVs and bacterial culture supernatants; however, did not promote OTII proliferation (Fig. 5b, c). Of note, proliferation triggered by HK EC-ova^{SECR} must occur from cleaved OVA peptides retained in the outer membrane because HK bacteria were extensively washed, and supernatants did not activate OTII cells. Incubation of BMDCs with different concentrations of sOVA and viable EC^{CTRL} showed no adjuvant effect of EC^{CTRL} on OTII proliferation further indicating that not the soluble antigen in presence of live bacteria but the membrane-association of antigens is required for the superior capacity to mediate antigen-specific T cell activation (Fig. 5d).

Overall, 10 µg sOVA triggered a similar proliferation in OTII cells than 5×10^6 live EC-ova^{OM} (that grow up to 2×10^7 bacteria per well till the addition of antibiotics after 90 min) and 2×10^9 HK EC-ova^{OM} (Fig. 5b, d). One EC-ova^{OM} expresses about 1×10^5 AIDA fusion proteins (I. Benz, unpublished data). The weight of an equimolar amount OVA$^{1\text{-}386}$ (45 kD) compared to the AIDA-OVA fusion proteins produced by 2×10^7 and 2×10^9 EC-ova^{OM} is 0.15 µg and 15 µg, respectively. That this calculation approximates the true concentrations is confirmed by WB analyses. 0.1 µg of sOVA showed an OVA-specific band that was slightly stronger than the band of 2×10^7 EC-ova^{OM} and slightly weaker than the band of 1×10^8 EC-ova^{OM} (Fig. 6a). These results revealed that viable EC-ova^{OM} induces similar OTII proliferation at about 100 times lower antigen concentrations than sOVA and HK EC-ova^{OM}. The WB in Fig. 6a also shows that EC-ova^{CYTO1} produces slightly more OVA than EC-ova^{OM}, which may explain the higher efficiency of HK EC-ova^{CYTO1} compared to HK EC-ova^{OM} to induce OTII proliferation (Fig. 6b).

Next, we asked whether antigen uptake of live or HK bacteria might be different. *E. coli* uptake into DCs was quantified by counting intracellular bacteria after LPS staining (Fig. 6b and Supplementary Figure 9). Uptake of HK *E. coli* were slightly inferior to the uptake of live *E. coli* although the difference was below a factor two (Fig. 6c) suggesting that this fact could not explain the different efficacies of antigen-specific OTII activation. Heat killing also did not cause significant antigen degradation, which was analyzed by IF staining of membranous OVA in EC-ova^{OM} (Fig. 6d) and WB analyses of lysates from live and HK bacteria EC-ova^{OM} and EC-ova^{CYTO1} (data not shown).

To further compare the antigen uptake of soluble antigens and antigens expressed in live *E. coli*, we loaded DCs with viable bacteria, bacterial lysates or different concentrations of sOVA followed by extensive washing of the extracellular medium after 90 min. Intracellular OVA was clearly detectable by WB after loading BMDCs with 50 µg/ml sOVA ($=10$ µg/200 µl) a concentration that induced the same amount of OTII proliferations as 2×10^6/200 µl live EC-ova^{OM}, which corresponds to the concentration used in this experiment. However, no OVA-specific band

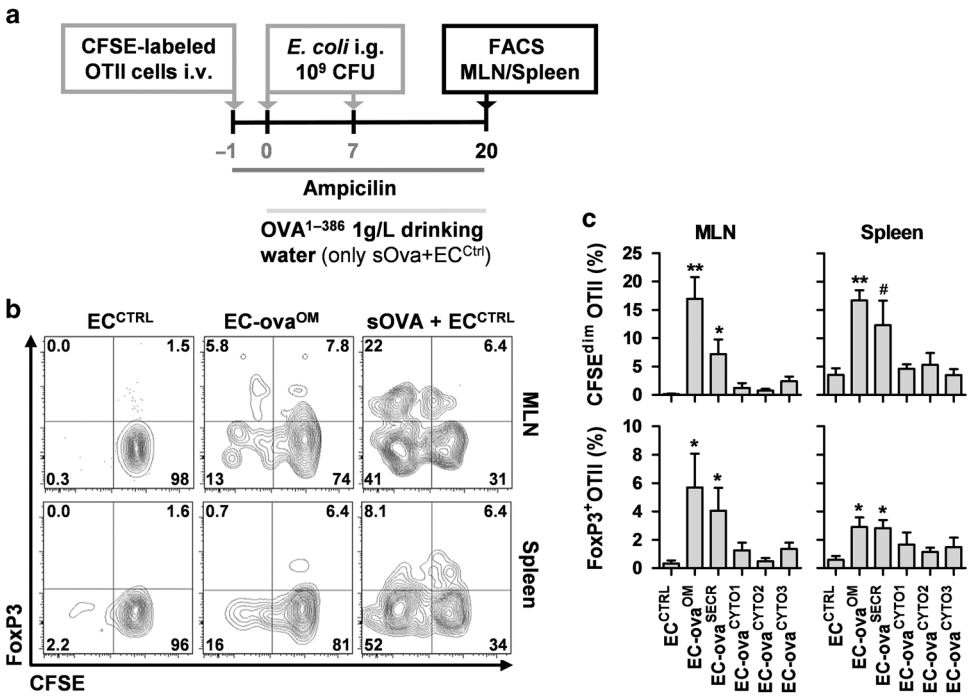

Fig. 4 EC-ova^{OM} and EC-ova^{SECR} induce expansion of antigen-specific T_{regs}. **a** Experimental setup. 1×10^7 CFSE-labeled CD45.2 OTII cells were adoptively transferred to CD45.1 mice 1 day prior to intestinal colonization with EC^{CTRL} or different EC-ova strains. **b** Representative FACS blots indicating proliferation and FoxP3 expression in OTII cells isolated from MLNs and spleens at day 20. For gating strategy see Supplementary Figure 8A. **c** Bar graphs represent mean ± SEM ($n = 5$–8 per condition) of proliferating and FoxP3-expressing OTII cells isolated from mice of indicated conditions at day 20. Statistical analysis was performed by one-way ANOVA and Dunn's post hoc test. *$p < 0.05$; **$p < 0.01$. # represents difference compared to EC^{CTRL} ($p < 0.05$) tested by Mann–Whitney *U* test

could be detected in cell lysates of DCs incubated with live or lysed EC-ova^{OM} or EC-ova^{CYTO1} (Fig. 6e). The band for the bacterial protein GroEL expressed at higher concentrations than the OVA fusion proteins was detectable in all conditions indicating uptake of bacterial proteins. The band was slightly weaker in the lysate conditions, although an exact quantification at this level was beyond the quality of the assay. Overall, these experiments suggest that the higher efficacy of activating antigen-specific T cells by live EC-ova^{OM} was not related to superior antigen uptake.

DISCUSSION

In this study we aimed to analyze whether the subcellular localization of antigens in commensal gut bacteria has a role for their ability to induce antigen-specific tolerance. Our initial hypothesis was that soluble or secreted antigens might be more effective in triggering tolerance and T_{reg} activation. Soluble antigens can be taken by APCs without the association of MAMPs, which have been suggested to be of advantage for the induction of a tolerogenic immune response. In turn, antigens that are physically associated with the commensal bacteria might be preferentially taken up together with immune-stimulatory MAMPs, which finally may favor a proinflammatory immune response.

To our surprise, our study proves that this hypothesis was wrong. We found that *E. coli* expressing OVA at the membrane were most effective in inducing the expansion of antigen-specific FoxP3$^+$ T_{regs} in MLNs and spleens and a systemic antigen-specific tolerance in a Th2-type allergic lung inflammation model. *E. coli* that cleaves the antigen from the intramembranous anchor protein was only slightly less effective; however, the results of our in vitro assays suggest that the tolerogenic effect is not mediated by the soluble antigen but by the fraction of cleaved OVA peptides that remain non-covalently associated with the bacterial cell wall. *E. coli* that express OVA in the cytoplasm had no effect on antigen-specific T_{reg} expansion and tolerance induction.

Membrane-associated OVA was about 100 times more efficient than soluble or cytoplasmic OVA in inducing antigen-specific CD4$^+$ T cell activation in vitro. Interestingly, this enhanced efficacy was lost when the bacteria were heat-killed. The higher efficiency of live EC-ova^{OM} was not related to different efficacies in antigen uptake by BDMCs that were used as APCs in the experiments. We were not able to quantify the antigen amounts in feces or tissue in the in vivo experiments. However, the contraction of sOVA in drinking water was 1 mg/ml corresponding to a molar antigen concentration of 22 µM. The concentration of EC-ova^{OM} in the colon was 6.9×10^8 bacteria/g corresponding to molar antigen concentration of 0.115 µM. This difference could explain why sOVA in drinking water induced tolerance and T_{reg} expansion with a similar or even higher efficacy than EC-ova^{OM}. Although not tested here, similar experiments in other studies have shown that lower concentrations of soluble antigens may not be sufficient to mediate oral tolerance.[32]

Although not formally excluded, it seems to be very unlikely that the use of AIDAc as surface-display carrier protein is mediating an adjuvant effect that may explain our findings. First, we tested in vitro soluble OVA with and without EC^{Ctrl} (that expresses AIDAc without OVA). However, EC^{Ctrl} did not enhance OTII proliferation. Furthermore, the loss of superior T cell activation efficacy of EC-ova^{OM} and EC-ova^{SECR} after heat killing does not coincide with the disappearance of AIDAc.

In contrast to our results, previous studies suggest that *E. coli* expressing model antigens do not always lead to immune tolerance upon intestinal colonization.[33,34] Lack of immune tolerance in these studies could be due to (i) clonal expansion of effector T cells in lymphopenic hosts and/or (ii) higher expression of the model antigen by the bacteria. Iqbal et al.[33]

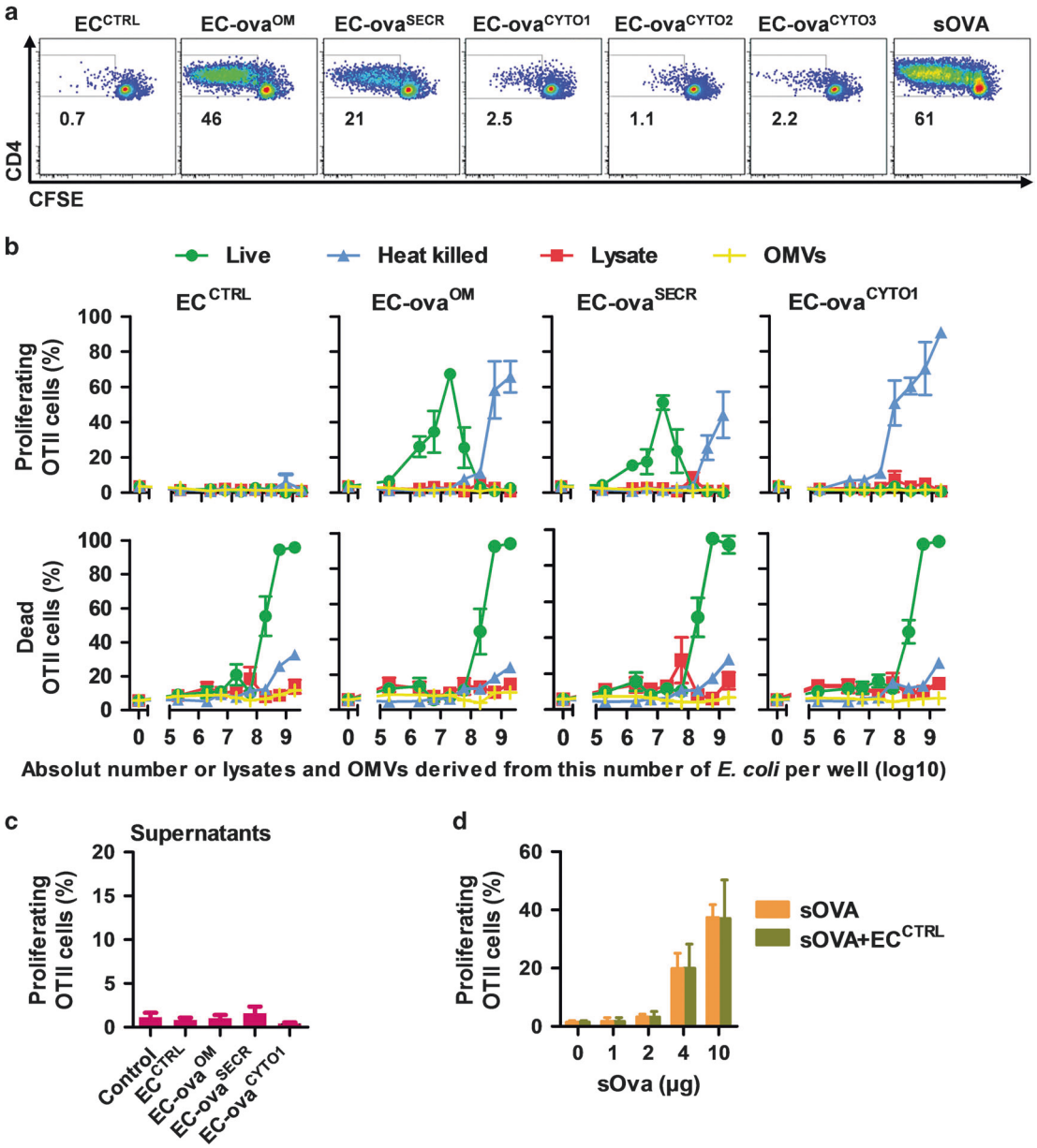

Fig. 5 Membrane-bound OVA of viable *E. coli* is highly efficient in activating antigen-specific $CD4^+$ cells. **a** 5×10^3 adherent BMDCs were co-cultured with 5×10^6 EC^{CTRL}, EC-ova^{OM}, EC-ova^{SECR}, EC-$ova^{CYTO1/2/3}$, or sOVA (10 µg) in 96-well plates in 200 µl medium. After 90 min, bacteria or sOVA were removed by washing three times. 200 µl medium containing 50 µg/ml gentamycin and 1×10^5 CFSE-labeled OTII T cells were added and co-cultured for 4 days. In the 90 min of BDMC/*E. coli* co-culture, bacterial numbers (intracellular + extracellular together) increased by approximately fourfold to 2×10^7 CFU (data not shown). At day 4, CFSE dilution in OTII cells was analyzed by FACS. Representative FACS plots of $n = 5$ experiments are shown. For gating strategy see Supplementary Figure 8B. **b** Dose-dependent effects on OTII proliferation (upper panel) and OTII cell death (HOECHST staining) of viable and heat-killed *E. coli*, bacterial lysates and outer membrane vesicles (OMVs). Numbers of viable *E. coli* correspond to the calculated number after 90 min of co-culture (input fourfold lower). Means ± SEM of two independent experiments performed in duplicates are shown. **c** Effects of bacterial culture supernatants (derived from OD_{595} ~0.5 cultures diluted 1:4 in cell culture medium) on OTII proliferation. **d** OTII proliferation induced by different concentration of sOVA ± 5×10^6 EC^{CTRL}. Means ± SEM of two experiments performed in duplicates are shown

expressed OVA in the cytoplasm of *E. coli*. However, the concentration of OVA within the bacteria was about 200 times higher than in our study. Clonal expansion of OVA-transgenic $CD4^+$ T cells adoptively transferred into Rag2−/− BALB/c mice was observed. These mice developed colitis upon transfer of in vitro primed Th1 and Th2 effector cells but not upon transfer of naive OVA-transgenic cells. Yoshida et al.[34] transformed *E. coli* with a high copy plasmid coding for secreted OVA. SCID or immunocompetent mice received antigen-naive OVA-transgenic T cells and were inoculated with 1×10^9 OVA-expressing *E. coli* per rectum every day. At day 4, SCID and immunocompetent BALB/c mice developed colitis paralleled by the expansion of Th1 and Th2-type OVA-specific effector T cells.

Westendorf et al. generated *E. coli* expressing an influenza virus hemagglutinin (HA) T cell epitope at the outer membrane.[35] However, colonization with this strain did not prevent diabetes in transgenic mice expressing both HA under the control of the insulin promoter on pancreatic β cells and HA-specific T cells. This result may suggest that tolerance towards *E. coli*-derived antigens is organ specific or most effective in Th2-type immunity.

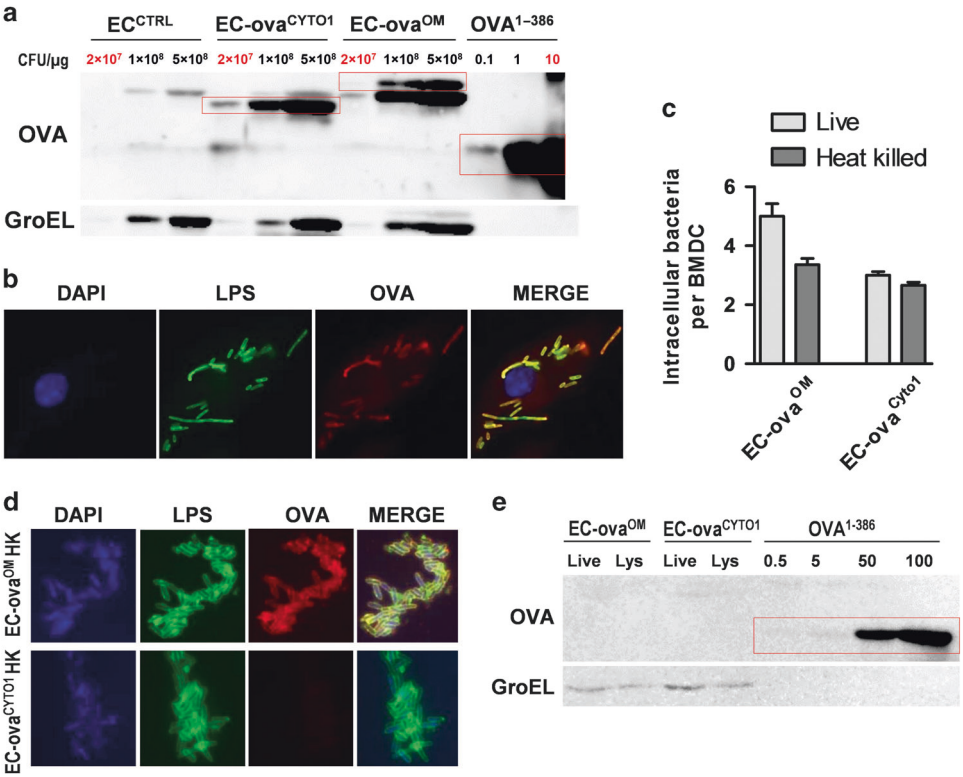

Fig. 6 Quantification of OVA uptake into BMDCs. **a** WB for OVA and GroEL of indicated bacterial lysates and sOVA. 2×10^7 bacteria and 10 µg of sOVA corresponds to the amounts used in the experiments described in 5A that induce a similar proliferative response in OTII cells. **b** IF for OVA (red), LPS (green), and DAPI (blue) of BMDCs challenged with EC-ova^{OM} for 20 min. Bar represents 10 µm. **c** Quantification of bacterial uptake into BMDCs. 1.5×10^5 BMDCs grown on coverslips were challenged with 1.5×10^6 live or heat-killed EC-ova^{OM} and EC-ova^{CYTO1} for 90 min in 200 µl of medium. Bacteria were counted after IF staining for LPS (green) and DAPI (blue) (see also Supplementary Figure 9). **d** IF for OVA (red), LPS (green) and DAPI (blue) of HK EC-ova^{OM} and HK EC-ova^{CYTO1}. **e** 3×10^6 BMDCs were incubated with 3×10^9 viable EC-ova^{OM} or EC-ova^{CYTO1}, lysates derived from 1.2×10^{10} EC-ova^{OM} or EC-ova^{CYTO1} or indicated concentrations of sOVA. After 90 min cells were washed three times and harvested. WB of cellular lysates for OVA and GroEL was performed

In contrast to these studies, Li et al.[36] reported that rectal inoculation of heat-killed *E. coli* expressing high doses of intracellular peanut allergens leads to downregulation of peanut specific IgE and hypersensitivity in a mouse model. However, the same treatment caused anaphylactic side effects in peanut allergic adults,[37] probably because of the high doses of allergens expressed by these bacteria that eventually were taken up systemically.

One important result of our study is that intestinal colonization with OVA-expressing *E. coli* induced systemic OVA-specific tolerance in a lung model. While local immunological tolerance prevents gut inflammation upon colonization, it remains to be determined which physiological function systemic tolerance towards commensal-derived antigens might have. We speculate that systemic tolerance to microbiota-derived antigens facilitate colonization of related commensals at other surfaces such as the upper airway, oral cavity, vagina, or skin. Furthermore, T cell receptors exhibit a high degree of cross-reactivity,[38] and several autoantigen-specific Abs and T cell receptors are cross-reactive towards commensal antigens.[39,40] Systemic tolerance to microbiota-derived antigens may prevent autoimmunity to cross-reactive autoantigens.

We did not use tolerogenic intestinal or MLN-derived DCs in the in vitro experiments. Hence, proliferation of OTII cells in vitro correlated with the production of IFNγ and IL-17A but not with the induction of FoxP3 expression (data not shown). The induction of a tolerogenic immune response with membrane-bound antigens in our study was probably mostly related to the model of intestinal colonization. Luminal gut bacteria are known to trigger T_{reg} responses, although the ratio of antigen-specific vs bystander activation has not been carefully studied.[41] Our in vitro experiments may suggest that also in responses to pathogens membrane-associated antigens are also more efficiently presented to effector T cells than cytoplasmic antigens. Although this has not been investigated in this study, the results of previous studies support this hypothesis. In vaccine development, it has been demonstrated that secreted or surface-located proteins are more likely to induce protective immune responses than intracellular proteins.[42] While protective B cell epitopes are likely to be expressed at the outer membrane, relatively little is known about how antigen localization affects the activation of MHC class II-restricted $CD4^+$ T cells. Priming of antigen-specific $CD4^+$ T cells was more efficient if cognate antigens were expressed at the surface of *Leishmania* and *Salmonella* rather than in their cytoplasm.[43–45] In mouse salmonellosis, $CD4^+$ responses against natural intracellular and surface antigens can be found, yet surface-expressed antigens confer better protection against lethal disease.[45] Interestingly, surface-located or secreted proteins of pathogens are depleted of peptide sequences predicted to bind to human MHC alleles. This might be a consequence of the evolutionary pressure for bacteria to eliminate sequences that elicit adaptive T cell immune responses.[46]

Our study shows the importance of antigen localization in addition to bacterial viability for the efficiency of T cell activation. However, the molecular mechanisms underlying our phenotypical findings remains largely unknown. Recently, bacterial RNA has been described as a viability-associated PAMP ('vita-PAMP'), the detection of which elicits distinct inflammatory immune

responses in APCs and promotes adaptive immunity in mice, pigs and humans.[47,48] We assume that vita-PAMP also contribute to the recognition of membrane-bound antigens of viable bacteria by $CD4^+$ T cells However, our results suggest that these putative vita-PAMPs and the antigen must physically be associated since the addition of live bacteria without OVA could not enhance the antigen-specific T cells proliferation in response to sOVA. To get access to intracellular antigens, bacteria must be lysed and therefore killed within phagolysosomes of APCs. During this process, vita-PAMPs might be inactivated resulting in less effective antigen processing and/or presentation. The preference of an adaptive immune responses towards surface antigens could be an important immune checkpoint for the detection of live and, hence, potential harmful bacteria.

Another result that mechanistically remains unexplained is the fact that antigens derived from bacterial lysates seem to have lower capacity to activate $CD4^+$ T cells than antigens derived from HK bacteria. Apart from the fact that antigen uptake from lysates into DCs might be inferior compared to antigen uptake from HK`bacteria, we may suggest the existence of immune-stimulatory effects of particle-associated antigens independently of MAMPs. Studies with nanoparticles showed that protein antigens covalently anchored to the surface of nanoparticles elicited an up to 1000-fold more efficient humoral and cellular immune response than soluble antigens. Costimulatory adjuvants inserted to the surface could enhance this effect but were not absolutely required, hence suggesting that surface-display of antigens on particles might enhance antigen presentation and immunogenicity independently of associated MAMPs.[49,50]

Our study uncovers new aspects of homeostatic T cell responses and shows the importance of subcellular antigen localization in the induction of immune tolerance towards viable gut commensals. Our results may provide opportunities for the development of new vaccine-based therapies. For example, probiotic strains expressing allergens or autoantigens could be designed as carriers for specific immunotherapy. Hence, we assume the low-dose surface-expressed antigens may offer a strategy to trigger T_{reg} responses with probably reduced immunogenic and anaphylactic side effects.

MATERIALS AND METHODS

Bacterial strains

The adhesin involved in diffuse adherence (AIDA-I)-surface-display system and the procedures used to generate OVA-expressing *E. coli* are summarized in Supplementary Figure 1 and Fig. 1a. AIDA-I from *E. coli* belongs to the group of type Va secretion system (T5aSS) autotransporters. Characteristically, all autotransporter systems contain a C-terminal β-domain forming a barrel-like structure in the outer membrane with a hydrophilic pore allowing passenger translocation across the outer membrane. The passenger domain in this study is replaced by the recombinantly expressed OVA peptide. The transporting linker region, connecting the passenger domain and the β-domain, harbors an autoproteolytic cleavage site that additionally enables to clip and release the OVA peptide to the extracellular surrounding.[26]

pOVA-pUC18[28] served as template for amplification of OVA for further cloning. PCR synthesis was performed for a 255-nucleotide sequence coding for the 85 aa $OVA^{256–340}$ peptide. DNA fragments obtained with the primer cloOva-4 and cloOva-5 (see Supplementary Table 1) were inserted through restriction by *Xma*I and *Kpn*I (Fermentas, St. Leon Rot, Germany) into the multiple cloning site (mcs) upstream of the membrane-embedded fraction of the AIDA-I proprotein (AIDAc) on the targeting vector pMK90 and pMK55.[26,51] The resulting plasmids were named $pOVA^{OM}$ and $pOVA^{SECR}$. DNA fragments obtained with the primer cloOva-6 and cloOva-7 (see Supplementary Table 1) were inserted through restriction by *BamH*I and *Hind*III (Fermentas) into the mcs downstream of MBP on the targeting vector pMAL-c2X. A PCR replication of the MBP-$OVA^{256–340}$ fusion construct was obtained using the primer cloOva-8 and cloOva-9 (see Supplementary Table 1) and ligated with a PCR replicon of the pMK90 backbone without the AIDAc transporter sequence (but with the AIDAc promoter) obtained using the primer cloOva10 and cloOva-11 (see Supplementary Table 1). The resulting plasmid was named $pOVA^{CYTO1}$. Correct insertions of all constructs were checked by sequencing (data not shown).

$pOVA^{OM}$, $pOVA^{SECR}$, $pOVA^{CYTO1}$, pOVA-pUC18,[28] pGex-OVA,[29] and pMK90 were transformed into a streptomycin-resistant *E. coli* K12 DH5α derivate to obtain EC-ova^{OM}, EC-ova^{SECR}, EC-ova^{CYTO1}, EC-ova^{CYTO2}, EC-ova^{CYTO3}, and EC^{CTRL}, respectively.

Western blot of bacterial lysates and supernatants

Bacteria from overnight cultures were washed twice with PBS containing protein inhibitors Complete mini (1 Tablet in 10 ml Buffer, Roche, Basel, Switzerland) and resuspended in 250 µl 1×PBS-Triton X100. The suspension was subjected four times to a freezing-thawing cycle and subsequently centrifuged (10 min, 10,000×*g*, 4 °C). Proteins were obtained from the supernatants and quantified with the Bradford method.

Bacterial culture supernatants for WB analysis were obtained after overnight culture and underwent a trichloroacetic acid precipitation. Supernatants were adjusted to a final trichloroacetic acid concentration of 10%, vortexed, and precipitated overnight at −20 °C. Proteins were ultracentrifuged for 20 min at 15,000 rpm, and pellets were air-dried at RT and resuspended in 6× loading dye (Lämmli buffer). 200-fold concentration was achieved; acid residues were titrated with 1 N NaOH in 1 µl steps.

Protein extracts (80 µg) were electrophoresed and then blotted following standard procedures. Primary Abs were specific for OVA, $AIDA^c$, MBP, and GroEL. Anti-rabbit IgG-HRP linked was used as secondary antibody (see Supplementary Figure 2). Blots were incubated 5 min with ECL solution (GE Healthcare, München, Germany), containing an HRP-substrate. Emission of a chemiluminescence signal was detected with a computer-assisted camera system (LAS4000, Fuji, Tokyo, Japan). Blots were stripped with 10 ml Stripping solution (Thermo Scientific) washed with TBS-T and reused.

Immunofluorescence (IF) and histology

Staining of bacteria was performed on Poly-L-Lysin precoated Shandon® Histo slides (Thermo Scientific, Waltham, MA, USA). A 0.01% solution was applied on the slides incubated for 5 min at RT and dried overnight. Bacteria were transferred by centrifugation with a Cytospin centrifuge (Shandon Labortechnik, Frankfurt am Main, Germany) and IF stainings were performed as described for tissue sections using anti-OVA pAb, anti-LPS-FITC and anti-AIDAc as primary Abs (see Supplementary Table 2).

Intestinal and lung tissues were fixed in Carnoy's solution and 4% PFA, respectively, before paraffin embedding. Tissue sections (2 µm) were deparaffinized, rehydrated, and subjected to haematoxylin and eosin (H&E) staining.

Pieces of intestinal tissues were frozen in Tissue-Tek O.C.T. Compound (Sakura, Alphen aan den Rijn, The Netherlands) at −80 °C. 7 µm cryosections were cut, transferred to superfrost slides, air-dried at RT, and fixed with prechilled acetone (−20 °C). After rehydration slides were blocked for 1 h at RT and a monospecific anti-OVA pAb was applied overnight at 4 °C. The next day, slides were incubated with an anti-rabbit IgG Alexa Fluor®594 secondary antibody for 1 h at RT in the dark. 2 µg/ml phalloidin-FITC (Sigma-Aldrich, #P5282) was added to stain actin filaments and samples were mounted with Vectashield® mounting medium containing nuclei dye DAPI (Vector Laboratories, Burlingame, CA, USA).

Samples were imaged with the Axio Imager Z1 (Zeiss, Jena, Germany).

Animals

Female C57BL/6 wild-type mice were purchased from Janvier (Orleans, France). C57BL/6 OTII C57BL/6 (B6.Cg-Tg(TcraTcrb) 425Cbn)/JCrl and C57BL/6 CD45.1 (B6.SJL-*Ptprc*^{a}*Pepc*^{b}/BoyCrl) mice were bred and housed in the University Hospital RWTH Aachen animal facility. The study was performed in agreement with the German animal protection law and was approved by the local animal care committee of the state North Rhine-Westphalia (LANUV, Germany; Aktenzeichen 84-02.04.2011.A171).

Intestinal colonization

Gastric application of bacteria (10^9 colony forming units [CFU] dissolved in 100 µl PBS) into 6-week-old mice was carried out under transient and volatile isoflurane anesthesia. Mice were pretreated with ampicillin in drinking water starting one day before gavage (1 g/l). Ampicillin-containing water was changed every 3 days during colonization. Stool sample homogenates were checked for the presence of bacteria on selective agar plates containing ampicillin and streptomycin. Control mice received soluble OVA (sOVA) 1% (w/v) (grade V, Sigma-Aldrich, St. Louis, MO, USA) in drinking water.

Fecal DNA isolation and quantitative real-time PCR

Total genomic DNA from approximately 20 mg snap frozen fecal pellets was isolated by Repeated-Bead-Beating (RBB) plus a column-based purification method as described in detail elsewhere.[52] For the enumeration of *E. coli* and total bacteria based on 16S rDNA gene sequences, all fecal samples were subjected to real-time PCRs (primer see Supplementary Table 1). Log10 plasmid copies per gram were achieved for each fecal sample from the cycle threshold values by using the constructed standard curves. The lower limit of detection was 2.73 log10 copies/g feces for *E. coli* and 5.04 log10 copies/g feces for the total bacteria load. Samples that were below the detection limit were included with zero plasmid copies.

OVA-induced allergic lung inflammation

For induction of allergic lung inflammation, mice were sensitized with 25 µg of the 85 aa OVA peptide (Selleckchem, Houston, USA) in 2% alum suspension subcutaneously in the lower right inguinal region. 13 day after senitization mice were challenged with inhaled OVA on three consecutive days. The following day mice were anaesthetized, blood was harvested, BAL performed and lung tissue obtained. For MC degranulation assay, a group of mice was immunized three times with intraperitoneal injection of 25 µg of the 85 aa OVA peptide in 2% alum (InvivoGen, Toulouse, France) suspension at days 0, 7, and 14. Serum was obtained at day 29 after OVA inhalation challenge.

Cell isolation

Spleens, mesenteric lymph nodes (MLNs), large, and small intestines were harvested from mice. Small and large intestines were cut into small pieces, extensively washed with complete tissue culture medium (CTCM = RPMI containing 10% FCS, 2 mM L-glutamine, 1 mM NaPyruvate, 55 nM β-mercaptoethanol, 25 mM HEPES) incubated with PBS containing 1% BSA, 5 mM EDTA, and 1 mM DTT (20 min, 37 °C) to remove mucus and epithelial cells and digested for 30 min at 37 °C in 5 ml CTCM medium containing 80 U/ml collagenase type 4 (Worthington, Freehold, NJ, USA) and 1250 Kunitz units/ml DNase 1 (Sigma-Aldrich). To obtain single cell suspensions, intestinal lamina propria tissue pieces as well as whole spleens and MLNs were filtered through a 70 µm cell strainer and subjected to red cell lysis (Red Cell Lysing Buffer; Sigma-Aldrich). $CD4^+$ OTII cells were purified from splenocytes and lymph nodes of OTII mice using the MACS $CD4^+$ T cell Isolation Kit according to the manufacturer's instructions (Miltenyi Biotec, Bergisch Gladbach, Germany)

Flow cytometry

Cells (max. 5×10^5) were incubated with fluorescent dye-coupled Abs against specific cell surface epitopes (see Supplementary Table 2) for 45 min at 4 °C in 50 µl PBS/BSA 1%. After washing, 1×10^4 APC beads for absolute cell counting (Calibrite APC beads, BD Bioscience, Franklin Lakes, NJ, USA) and 1 µg/ml Hoechst 33342 dye (Sigma-Aldrich) for live/dead cell differentiation was added. FoxP3 staining was performed using the FoxP3/Transcription Factor Fixation/Permeabilization Concentrate and Diluent (ebioscience, Frankfurt am Main, Germany) according to manufacturer's recommendations. Flow cytometric measurements were performed on BD FACS Canto II (BD Biosciences). Data were analyzed using FlowJo 7.6.5 (FlowJo, LLC, San Carlos, OR, USA).

RNA isolation and RT-PCR

RNA was isolated from colonic and lung tissue using peqGOLD-RNAPure® reagent (Peqlab, Erlangen, Germany) according to the manufacturer's instructions. cDNA was transcribed with the Omniscript RT kit (Qiagen, Hilden, Germany) and amplified with the SYBRGreen PCR Master Mix (Applied Biosystems, Foster City, CA, USA) and gene-specific primers (see Supplementary Table 1) in the ABI PRISM 7300 sequence detection system (Applied Biosystems). Data were analyzed by the ΔΔCt method using *Gapdh* for normalization.

Enzyme-linked immunosorbent assay (ELISA) for serum anti-OVA Abs

Microtiter plates were coated overnight at 4 °C with 50 µl of sOVA 10 µg/ml in pH 9.6 carbonate buffer. BSA-coated plates were used for analyzing non-specific binding. After each incubation step, plates were washed four times with 200 µl of PBS/BSA 0.1%/TWEEN 0.05% (TBS-T). Plates were blocked with 200 µl PBS/BSA 5% for 1 h. Mice sera were diluted in PBS/BSA 1% for determination of IgG1 (dilution $1:1 \times 10^3$, $1:1 \times 10^4$, $1:1 \times 10^5$, $1:1 \times 10^6$) and IgG2b (dilution 1:20, 1:100, 1:500). An 11-point twofold serial dilution curve of sera with a high anti-OVA Ab titer derived from mice sensitized two times with OVA in Complete Freund's adjuvant served as a standard. Experimental sera and standard were incubated overnight at 4 °C. Secondary biotinylated antibody (see Supplementary Figure 2) was added for 2 h at RT, plates were washed and 50 µl HRP solution (1:200, R&D Systems, Minneapolis, MN, USA) was added 40 min. Afterwards, 200 µl TMB substrate solution (1 Tablet 3,3′,5,5′-Tetramethylbenzidine (Sigma & Aldrich) dissolved in 1 ml DMSO 30–60 min; 9.5 ml 0.05 M Citrate/Phosphate solution; 30 µl of 30% hydrogen peroxide solution per 10 ml) was incubated for 10–15 min and monitored meanwhile. The reaction was stopped by adding 50 µl stop solution 2 N sulfuric acid (H_2SO_4) and the extinction was measured at OD 450 nm. Titers of the standard serum were defined as the highest dilution giving twice the background absorbance. Titers of samples were indirectly calculated by comparing OD values of the highest serum dilution above the twofold background level to the standard curve.

Mast cell degranulation assay

Bone marrow cells (1×10^6/ml) from 6- to 8-week-old mice (C57BL/6) were cultured (37 °C, 5% CO_2) in CTCM containing 2% X63Ag8-653-conditioned medium as a source of IL-3 and 1% CHO-conditioned medium as a source of Stem cell factor (SCF). At weekly intervals, the nonadherent cells were reseeded at 5×10^5 cells/ml in fresh medium. By 4 weeks in culture, more than 90% of the cells were ckit, IL-33R and FceRI positive as assessed by FACS. For the degranulation assay, 3×10^5 BMMCs in 80 µl Tyrode's buffer (10 mM HEPES, 130 mM NaCl, 6.2 mM D-glucose, 3.0 mM KCl, 1.4 mM $CaCl_2$, 1.0 mM $MgCl_2$, and 0.1% BSA) were plated in 96-well plates and kept for 15 min at 37 °C. Cells were then stimulated for 30 min at 37 °C with 20 µl mouse sera and antigen (sOVA 100 ng/ml) as indicated. After incubation, cells were

stored for 5 min on ice followed by centrifugation at 1000×*g* for 10 min to harvest cell supernatants and pellets. For cell lysis, pellets were treated with 80 µl Tyrode's + 0.5% NP40 for 10 min on ice. Cell debris were removed by centrifugation (3500×*g*, 10 min). For measurement of β-hexosaminidase activity, 20 µl of supernatants and lysates were incubated in 96-well plates with 50 µl substrate solution (3.7 mM *p*-nitrophenol-*N*-acetyl-β-D-glucosaminide; 0.1 M Na-citrate pH 4.5) for 90 min at 37 °C. 150 µl stopping solution (0.2 M Glycine, pH 10.7) was added and absorption at 405 nm was determined. Degranulation in the supernatant was calculated as % of total cellular (lysate + supernatant) β-hexosaminidase content.

Adoptive transfer experiments

OTII cells were labeled with 5 µM CFSE using Vybrant® CFDA SE Cell Tracer Kit (Invitrogen, Karlsruhe, Germany) in PBS/FCS 0.5% for 5 min at room temperature (RT). 1×10^7 CFSE-labeled cells were transferred intravenously to congenic CD45.1 mice 1 day prior to intestinal colonization with EC^{CTRL}, EC-ova^{OM}, EC-ova^{SECR} or EC-$ova^{CYTO1/2/3}$. Control animals were fed with soluble sOVA (1% (w/v) in drinking water). At day 20 spleens and MLN cells were isolated for FACS analysis.

In vitro co-culture experiments

For in vitro experiments, *E. coli* were cultured in LB medium overnight and subsequently washed three times with PBS. For heat killing, *E. coli* were incubated at 75 °C for 60 min. Complete killing was tested by plating. Bacterial lysates were produced by sonication. Supernatants were harvested from late log phase (OD_{595} ~0.5) cultures after centrifugation (5 min, 10,000×*g*). Lysates and supernatants were filtered through a 0.2 µm syringe filter to remove remaining intact bacteria.

OMVs were isolated from overnight cultures as described.[53] Cells were briefly pelleted at 10,000×*g* for 10 min at 4 °C and supernatants were filtered through 0.45 µm filter membrane (Millipore Durapore PDF membrane). OMVs were pelleted by centrifugation for 3 h at 38,400×*g* at 4 °C and resuspended in DPBS supplemented with 0.2 M NaCl. OMVs were filter sterilized with 0.45 µm Ultra-free spin filters (Millipore).

For the generation of BMDCs, bone marrow was flushed from mice femur and bone marrow cells (2×10^6/10 ml in a 10 cm dish) from 6- to 8-week-old mice (C57BL/6) were cultured (37 °C, 5% CO_2) in CTCM supplemented with 10% R1 cell-conditioned medium, as a source of GM-CSF corresponding to 200 U/ml. Every 3 days, cells were reseeded at 2×10^5 cells/ml in fresh medium. By 10 days in culture, more than 90% of the cells were CD11c and CD11b positive as assessed by FACS.

For the assessment of antigen presentation of OVA expressed by *E. coli*, 5×10^3 BMDCs were cultured overnight in 96-round bottom well plates containing CTCM. The next day, adherent BMDCs were washed two times and loaded with 200 µl CTCM containing live *E. coli* (in medium without antibiotics), HK *E. coli*, bacterial lysates, OMVs, bacterial supernatants, or sOVA at indicated concentrations. After 90 min, medium was removed, cells were washed three times and 1×10^5 MACS-purified and CFSE-labeled OTII cells were added in 200 µl CTCM containing 50 µg/ml gentamycin to stop extracellular bacterial growth. At day 4 of co-culture, proliferation (=CFSE dilution) was assessed by FACS.

Statistics

Data are expressed as means (±SEM), median or logarithmic mean as indicated. Boxes and whiskers indicate median, 10/25/75/90 percentiles and outliers as dots. Statistical significances were analyzed by Mann–Whitney *U* test for comparison of two groups or by one-way ANOVA followed by Dunn's post hoc test for the comparison of multiple groups. Statistical analyses were performed using GraphPad Prism (GraphPad Software, Inc., La Jolla, CA, USA).

ACKNOWLEDGEMENTS

We thank Ursula Schneider for help with the lung histological sections; Andreas Ludwig and Andrea Koenen for help with allergic lung inflammation model; Michael Huber and Marlies Kaufmann for providing X63Ag8-653-conditioned medium for mast cell culture; Mary Jo Wick for providing pOVA-pUC18; Joao G. Magalhaes for providing pGex-OVA, and Claude Parsot for discussion regarding the strategy of OVA expression in *E. coli*. This work was supported by the German Research Foundation (DFG SE 1122/1 and SFB985 / C3) and the European Union's Seventh Framework Programme (FP7/2007-2013) under Grant Agreement No. 305564 (SysmedIBD).

AUTHOR CONTRIBUTIONS

Conceived and designed the experiments: E.B., O.P., G.S. Performed the experiments: E.B., A.D.M., J.V., S.R. Advise in construction of OVA-expressing *E. coli*: T.K., I.B. Data analysis: E.B., G.S. Wrote the paper: E.B., J.V., O.P., C.T., G.S.

ADDITIONAL INFORMATION

The online version of this article (https://doi.org/10.1038/s41385-018-0061-0) contains supplementary material, which is available to authorized users.

Competing interests: The authors declare no competing interests.

REFERENCES

1. Buttó, L. F., Schaubeck, M. & Haller, D. Mechanisms of microbe-host interaction in Crohn's disease: dysbiosis vs. pathobiont selection. *Front. Immunol.* **6**, 555 (2015).
2. Sellge, G. & Kufer, T. A. PRR-signaling pathways: learning from microbial tactics. *Semin. Immunol.* **27**, 75–84 (2015).
3. Wesemann, D. R. & Nagler, C. R. The microbiome, timing, and barrier function in the context of allergic disease. *Immunity* **44**, 728–738 (2016).
4. Bischoff, S. C. & Sellge, G. *Food Allergy Adverse Reaction to Foods Food Additives* 5th edn 16–30 (Blackwell Publishing Ltd, Oxford, UK, 2014).
5. Cerovic, V., Bain, C. C., Mowat, A. M. & Milling, S. W. F. Intestinal macrophages and dendritic cells: What's the difference? *Trends Immunol.* **35**, 270–277 (2014).
6. Toit, G. Du et al. Randomized trial of peanut consumption in infants at risk for peanut allergy. *N. Engl. J. Med.* **372**, 803–813 (2015).
7. Worbs, T. Oral tolerance originates in the intestinal immune system and relies on antigen carriage by dendritic cells. *J. Exp. Med.* **203**, 519–527 (2006).
8. Yang, Y. et al. Focused specificity of intestinal TH17 cells towards commensal bacterial antigens. *Nature* **510**, 152–156 (2014).
9. Lécuyer, E. et al. Segmented filamentous bacterium uses secondary and tertiary lymphoid tissues to induce gut IgA and specific T helper 17 cell responses. *Immunity* **40**, 608–620 (2014).
10. Goto, Y. et al. Segmented filamentous bacteria antigens presented by intestinal dendritic cells drive mucosal Th17 cell differentiation. *Immunity* **40**, 594–607 (2014).
11. Atarashi, K. et al. Treg induction by a rationally selected mixture of *Clostridia* strains from the human microbiota. *Nature* **500**, 232–236 (2013).
12. Kuhn, K. A. & Stappenbeck, T. S. Peripheral education of the immune system by the colonic microbiota. *Semin. Immunol.* **25**, 364–369 (2013).
13. Flannigan, K. L. et al. IL-17A-mediated neutrophil recruitment limits expansion of segmented filamentous bacteria. *Mucosal Immunol.* **10**, 673–684 (2017).
14. Kumar, P. et al. Intestinal interleukin-17 receptor signaling mediates reciprocal control of the gut microbiota and autoimmune inflammation. *Immunity* **44**, 659–671 (2016).
15. Atarashi, K. et al. Th17 cell induction by adhesion of microbes to intestinal epithelial cells. *Cell* **163**, 367–380 (2015).
16. Atarashi, K. et al. Induction of colonic regulatory T cells. *Science* **331**, 337–342 (2011).
17. Sarrabayrouse, G. et al. CD4CD8αα lymphocytes, a novel human regulatory T cell subset induced by colonic bacteria and deficient in patients with inflammatory bowel disease. *PLoS Biol.* **12**, e1001833 (2014).
18. Round, J. L. & Mazmanian, S. K. Inducible Foxp3+ regulatory T-cell development by/na commensal bacterium of the intestinal microbiota. *Proc. Natl Acad. Sci. USA* **107**, 12204–12209 (2010).
19. Jeon, S. G. et al. Probiotic bifidobacterium breve induces IL-10-producing Tr1 cells in the colon. *PLoS Pathog.* **8**, 1–15 (2012).
20. Geuking, M. B. et al. Intestinal bacterial colonization induces mutualistic regulatory T cell responses. *Immunity* **34**, 794–806 (2011).
21. Arpaia, N. et al. Metabolites produced by commensal bacteria promote peripheral regulatory T-cell generation. *Nature* **504**, 451–455 (2013).

22. Furusawa, Y. et al. Commensal microbe-derived butyrate induces the differentiation of colonic regulatory T cells. *Nature* **504**, 446–450 (2013).
23. Lathrop, S. K. et al. Peripheral education of the immune system by colonic commensal microbiota. *Nature* **478**, 250–254 (2011).
24. Huibregtse, I. L. et al. Induction of ovalbumin-specific tolerance by oral administration of *Lactococcus lactis* secreting ovalbumin. *Gastroenterology* **133**, 517–528 (2007).
25. Blander, J. M. & Medzhitov, R. Toll-dependent selection of microbial antigens for presentation by dendritic cells. *Nature* **440**, 808–812 (2006).
26. Buddenborg, C. et al. Development of a tripartite vector system for live oral immunization using a Gram-negative probiotic carrier. *Int. J. Med. Microbiol.* **298**, 105–114 (2008).
27. Robertson, J. M., Jensen, P. E. & Evavold, B. D. DO11.10 and OT-II T cells recognize a C-terminal ovalbumin 323-339 epitope. *J. Immunol.* **164**, 4706–4712 (2000).
28. Yrlid, U. & Wick, M. J. Antigen presentation capacity and cytokine production by murine splenic dendritic cell subsets upon Salmonella encounter. *J. Immunol.* **169**, 108–116 (2002).
29. Neophytou, P. I. et al. Development of a procedure for the direct cloning of T-cell epitopes using bacterial expression systems. *J. Immunol. Methods* **196**, 63–72 (1996).
30. Jaumouillé, V., Francetic, O., Sansonetti, P. J. & Tran Van Nhieu, G. Cytoplasmic targeting of IpaC to the bacterial pole directs polar type III secretion in Shigella. *EMBO J.* **27**, 447–457 (2008).
31. Donaldson, G. P., Lee, S. M. & Mazmanian, S. K. Gut biogeography of the bacterial microbiota. *Nat. Rev. Microbiol.* **14**, 20–32 (2016).
32. Lamont, A. G., Mowat, A. M. & Parrott, D. M. V. Priming of systemic and local delayed-type hypersensitivity responses by feeding low doses of ovalbumin to mice. *Immunology* **66**, 595–599 (1989).
33. Iqbal, N. et al. T helper 1 and T helper 2 cells are pathogenic in an antigen-specific model of colitis. *J. Exp. Med* **195**, 71–84 (2002).
34. Yoshida, M. et al. Differential localization of colitogenic Th1 and Th2 cells monospecific to a microflora-associated antigen in mice. *Gastroenterology* **123**, 1949–1961 (2002).
35. Westendorf, A. M. et al. Intestinal immunity of *Escherichia coli* NISSLE 1917: a safe carrier for therapeutic molecules. *FEMS Immunol. Med. Microbiol.* **43**, 373–384 (2005).
36. Li, X. M. et al. Persistent protective effect of heat-killed Escherichia coli producing 'engineered,' recombinant peanut proteins in a murine model of peanut allergy. *J. Allergy Clin. Immunol.* **112**, 159–167 (2003).
37. Wood, R. A. et al. A phase 1 study of heat/phenol-killed, *E. coli*-encapsulated, recombinant modified peanut proteins Ara h 1, Ara h 2, and Ara h 3 (EMP-123) for the treatment of peanut allergy. *Allergy Eur. J. Allergy Clin. Immunol.* **68**, 803–808 (2013).
38. Birnbaum, M. E. et al. Deconstructing the peptide-MHC specificity of T cell recognition. *Cell* **157**, 1073–1087 (2014).
39. Ruff, W. E., Haven, N. & Kriegel, M. A. The role of the gut microbiota in the pathogenesis of antiphospholipid syndrome. *Curr. Rheumatol. Rep.* **17**, 472 (2015).
40. Verdier, J., Luedde, T. & Sellge, G. Biliary mucosal barrier and microbiome. *Viszeralmedizin* **31**, 156–161 (2015).
41. Tanoue, T., Atarashi, K. & Honda, K. Development and maintenance of intestinal regulatory T cells. *Nat. Rev. Immunol.* **16**, 295–309 (2016).
42. Mayers, C. et al. Analysis of known bacterial protein vaccine antigens reveals biased physical properties and amino acid composition. *Comp. Funct. Genom.* **4**, 468–478 (2003).
43. Hess, J. et al. Superior efficacy of secreted over somatic antigen display in recombinant Salmonella vaccine induced protection against listeriosis. *Proc. Natl Acad. Sci. USA* **93**, 1458–1463 (1996).
44. Prickett, S. et al. In vivo recognition of ovalbumin expressed by transgenic *Leishmania* is determined by its subcellular localization. *J. Immunol.* **176**, 4826–4833 (2006).
45. Barat, S. et al. Immunity to intracellular salmonella depends on surface-associated antigens. *PLoS Pathog.* **8**, e1002966 (2012).
46. Halling-Brown, M., Sansom, C. E., Davies, M., Titball, R. W. & Moss, D. S. Are bacterial vaccine antigens T-cell epitope depleted? *Trends Immunol.* **29**, 374–379 (2008).
47. Ugolini, M. et al. Recognition of microbial viability via TLR8 drives TFHcell differentiation and vaccine responses. *Nat. Immunol.* **19**, 386–396 (2018).
48. Sander, L. E. et al. Detection of prokaryotic mRNA signifies microbial viability and promotes immunity. *Nature* **474**, 385–389 (2012).
49. Bershteyn, A. et al. Robust IgG responses to nanograms of antigen using a biomimetic lipid-coated particle vaccine. *J. Control. Release* **157**, 354–365 (2012).
50. Irvine, D. J., Hanson, M. C., Rakhra, K. & Tokatlian, T. Synthetic nanoparticles for vaccines and immunotherapy. *Chem. Rev.* **115**, 11109–11146 (2015).
51. Casali, N., Konieczny, M., Schmidt, M. A. & Riley, L. W. Invasion activity of a *Mycobacterium tuberculosis* peptide presented by the *Escherichia coli* AIDA autotransporter. *Infect. Immun.* **70**, 6846–6852 (2002).
52. Salonen, A. et al. Comparative analysis of fecal DNA extraction methods with phylogenetic microarray: effective recovery of bacterial and archaeal DNA using mechanical cell lysis. *J. Microbiol. Methods* **81**, 127–134 (2010).
53. Manning, A. J. & Kuehn, M. J. Contribution of bacterial outer membrane vesicles to innate bacterial defense contribution of bacterial outer membrane vesicles to innate bacterial defense. *BMC Microbiol.* **258**, 605–619 (2011).